Smart Grid Line Event Classification Using Supervised Learning Over PMU Data Streams

Duc Nguyen*, Richard Barella*, Scott A. Wallace*, Xinghui Zhao* and Xiaodong Liang†
*School of Engineering and Computer Science
Washington State University Vancouver
Vancouver, WA 98686
Email: {duc.nguyen,richard.t.barella,wallaces,x.zhao}@wsu.edu
†Department of Electrical and Computer Engineering
Memorial University of Newfoundland
St. John's, NL A1B 3X5
Email: xliang@mun.ca

***Abstract*—Emerging smart grid technology offers the possibility of a more reliable, efficient, and flexible energy infrastructure. A core component of the smart grid are phasor measurement units (PMUs) which offer the ability to capture time-coherent measurements across a geographically distributed area. However, due to the fast sampling rate of these devices, a significant volume of data is generated on a daily basis and this presents challenges for how to leverage the information most effectively. In this paper, we address this challenge by applying machine learning techniques to PMU data for the purpose of detecting line events in a wide-area power grid. Specifically, we use archived synchrophasor data from PMUs located across the Pacific Northwest to train and test a decision tree built using the J48 algorithm. In contrast to other studies exploring machine learning in the context of the smart grid, our work uses PMU data from a large, active, power grid as opposed to data obtained from a simulation. We show that our classifier performs as well as hand-coded rules developed by a domain expert when applied at locations near to a line fault and that it significantly outperforms hand-coded rules when identifying line faults from a distance.**

Keywords*—smart grids; phasor measurement units; machine learning; event detection; decision trees

I. Introduction

With the advancement of digital communication and control technologies and their application in the power grid, the smart grid has become a major research and development area in which the ultimate goal is to achieve dynamic optimization of the grid's operation and resources. The key technologies in the smart grid include integrated communication across the grid, advanced control methods, and techniques in sensing, metering and measurement [1]. Sensing, metering and measurement are critical, as they can be used to enhance integrated communication and advanced control.

Synchrophasor technology has attracted significant attention from academia and from the power industry since its first introduction in 1980s [2]. A key feature provided by this technology is the ability to synchronize critical measurements from widely disbursed geographical locations in a power grid with a precise clock through the global positioning system (GPS). With the precise time-stamping of each data point and alignment to a common time reference provided by GPS, time coherent measurements can be obtained throughout the wide area of a power grid [3]. This, in turn, enables the grid operators to accurately analyze the operating status of the grid at large.

The device used to measure synchrophasors is known as the phasor measurement unit (PMU). PMUs are able to measure synchronized voltage and current phasors, frequency, and rate of change of frequency. The rate at which measurements are stored and reported ranges from 10–60 samples per second for a 60 Hz system [4]. A PMU's sampling and recording rate is much higher than conventional monitoring technologies such as supervisory control and data acquisition (SCADA), which measure once every two to four seconds [5] [6]. Therefore, the measurements from PMUs offer finer-grained real-time data from a power grid, providing the potential for developing applications which benefit the overall grid operation and planning. Such applications generally fall in three categories: 1) providing wide-area visualization and situation awareness; 2) response-based automated control to improve reliability and efficiency 3) improving system planning and system analysis by conducting power system performance baselining, model validation, and event analysis [5]–[8]. Since most of the blackouts of a power grid are usually caused by a single event which leads to cascading outages [9], it is critical to accurately and efficiently detect these line events before severe consequences happen. It has been shown that 50% of power system faults occur in the transmission and distribution lines [10]. PMUs that are deployed on transmission lines provide great opportunity for detecting those line events. In this paper, we present an approach for event detection based on PMU data. The objective of this approach is to detect and classify line events from PMU data streams. These events include Single Line to Ground, Line to Line, and Three Phase faults.

Although the high sampling frequency of PMUs provides potentials for event detection, it also presents challenges for data processing, due to the volume of the data [11]. A typical PMU can measure 16 phasors with a 32-bit floating point

This work is partially supported by the DoE / Bonneville Power Administration through the Technology Innovation Program: (TIP #319).

978-1-5090-0172-9/15/$31.00

value for phasor magnitude and another for phasor angle. This, combined with an 8 byte time stamp, 2 byte status flag, and 8 more bytes for frequency and rate of frequency change represents a minimal set of signals that would be desirable to archive. Recording samples at 60Hz, a single such PMU creates 5,184,000 samples per day or roughly 721MB per PMU per day. Our dataset, from the Bonneville Power Administration's PMU installation in the Pacific Northwest, contains data from approximately 44 PMUs (generating roughly 1TB per month) and the installed base continues to grow. In order to leverage the PMU data for event detection, we must be able to store, access, and process, large data sets efficiently. While individual power systems engineers may have been capable of processing smaller data sets from a few PMUs completely manually, we believe that leveraging all the latent information in tomorrow's PMU data will require machine learning approaches [12].

In this paper, we focus on automatically detecting and classifying line events in live or archived PMU data using machine learning with the goal of replacing hand-built classification rules developed by domain experts. In the remainder of this paper we proceed as follows. In Section II, we examine related work that uses machine learning in conjunction with real or simulated PMU data focusing on machine learning for event detection. In Section III, we describe our previous work to develop a fault detection technique using hand-built classification rules based on measurements from 11 months of archived PMU data from the Pacific Northwest. This approach serves as a baseline to evaluate the performance of subsequent classifiers built using machine learning. In Section IV, we describe our dataset and test metrics. In Section V, we compare the performance of the domain expert's hand built classification rules against the rules generated through decision tree learning using a set of unexamined test data. Finally, in Section VI, we conclude with a summary of the project and directions for future work.

II. Related Work

PMUs are widely used to monitor the operational status of a power grid with the aim of enhancing the situation awareness for power system operators. A significant amount of work has been done to detect or monitor certain conditions of a power grid by leveraging information extracted from PMU data. Jiang et al. propose an online approach for fault detection and localization using SDFT (smart DFT) [13]. Liu et al. use Frequency Domain Decomposition for detecting oscillations [14]. Kazami et al. propose a multivariable regression model to track fault locations [15]. Besides voltage and current magnitudes, which are the most commonly used features in detecting faults, phase angle measurements can also be used in detecting outages [16].

Most recently, with the emergence of big data analytics, new technologies are introduced to PMU data storage and processing, such as Hadoop [17], and data cloud [18]. Most importantly, a variety of machine learning techniques have been applied to analyze PMU data for the purpose of recognizing patterns or signatures of events. Antoine et al. propose to identify causes for inter-area oscillations by clustering a number of parameters provided by PMUs, including mode frequency, the voltage angle differences between areas and the mode shapes [19]. It has been shown that by clustering these parameters, changes in inter-area oscillations can be explained. Clustering methods with unsupervised learning do not require labeled training data, however, once the clusters are generated, an expert's knowledge is often needed to interpret and compare the clusters [19].

In contrast to clustering, classification methods employ supervised learning and therefore, after training, can identify known signatures or patterns without domain knowledge from experts. The work presented in this paper falls in this category. Zhang et al. propose a classification method for finding fault locations based on pattern recognition [20]. The key idea is to distinguish a class from irrelevant data elements using linear discriminant analysis. The classification is carried out based on two types of features: nodal voltage, and negative sequence voltage. Similar classification techniques are used to detect voltage collapse [21] and disturbances [22] in power systems. Specifically, Diao et al. develop and train a decision tree using PMU data to assess voltage security [21]. Ray et al. build Support Vector Machines and decision tree classifiers based on a set of optimal features selected using a genetic algorithm [22]. Support Vector Machine-based classifiers can also be used to identify fault locations [23], and predict post-fault transient stability [24]. Although classification approaches are effective in grouping a data element into one of several predefined categories, they are not sufficient to make continuous valued decisions. In this case, regression trees can be used. For example, a regression tree based approach is used for predicting stability margin, i.e., how far the system is away from a disturbance [25]. Regression trees have also been used for on-line dynamic security assessment under the impact of missing PMU data [26].

In addition, several different basic machine learning techniques can be combined to perform a multi-stage task. Al Karim et al. propose a three-stage approach for fault analysis [27]. Specifically, in the first stage, a K-nearest neighbor algorithm is used to find patterns in a fault and classify it. Then in stage 2, a Naive Bayes algorithm is used to find out the most frequent fault in the dataset. In the last step, a K-means clustering algorithm is applied to both system data and classified data, in order to recognize patterns (similarities).

Although a variety of machine learning techniques have been proposed to analyze PMU data for event detection and prediction, very few have been applied to real PMU data collected from a large-scale Wide Area Measurement System (WAMS). Gomez et al. apply a SVM based algorithm to a model of practical power system [24]. However, the number of PMUs considered is restricted to 15. All other approaches mentioned in this Section are based on simulations.

In this paper, we present our experience of mining real PMU data collected from Bonneville Power Administration's (BPA's) transmission grid. Our data set includes signals from 44 PMUs over a one year period (October 2012 through September 2013) and reflects real system responses under various fault conditions. While simulation data can be used when real measurements are limited or unavailable, there is inherently some uncertainty in the simulation model's accuracy which can provide wrong or misleading data [28]. Thus, real PMU data from a large power grid is best source for machine learning purposes as it captures the most accurate representation of the target power system.

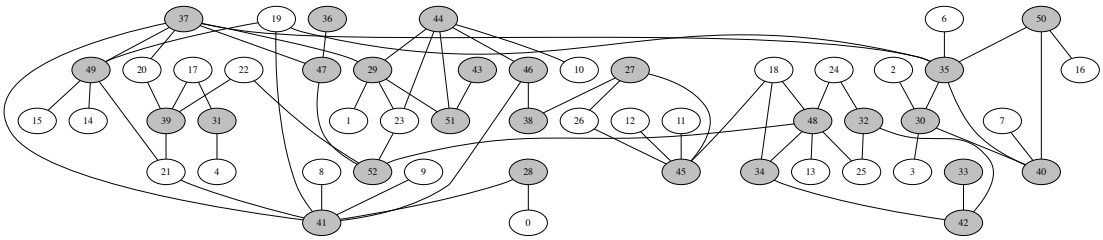

Fig. 1. PMU topology: nodes indicate substation sites (shaded nodes indicate PMU locations); edges indicate transmission lines instrumented with a PMU.

III. Background

In 2014, we developed a method for identifying Single Line to Ground faults using hand-coded rules applied to PMU data streams [29]. Recently, we extended this approach to detect three types of line faults: Single Line to Ground (SLG), Line to Line (LL) and Three Phase (3P) faults. Voltages of each phase (A, B and C) are normalized by their steady state values into the so called *per unit* system (see Figure 2). At each point in time, the voltage measurements of each of the three phases are subjected to classification rules to look for a significant deviation that may signal a fault.

For these *expert-defined* rules, thresholds for each fault type were determined from a theoretical foundation and supported by manually examining archival PMU data provided by Bonneville Power Administration. The event dataset includes the time and location of all known line events that occurred during an 11 month period on all of BPA's transmission lines instrumented with at least one PMU. At the time, BPA had PMUs in operation at 34 substations. PMUs are typically set to measure voltage at the substation bus (often multiple busses) and current on individual transmission lines, although in some cases voltage is also measured for transmission lines. Figure 1 illustrates the network topology, giving a general idea about the connectivity between PMUs. Note that site names have been replaced with generic labels at the request of BPA and transmission lines that are not monitored by a PMU are not shown. Shaded nodes represent substations with a PMU. Thus, for example, the transmission line connecting sites 38 and 27 is monitored on each end of the line, while the transmission line connecting sites 27 and 26 is monitored only on one side.

Our manual examination of this dataset began by generating voltage plots and statistics for each event. BPA verified the accuracy of this fault list and was able to further verify the specific type of event in the majority of cases (60 faults total). PMU measurements from these faults were used to set thresholds on the hand-built classification rules and for the machine learning tasks described in Section IV. BPA's PMUs record measurements at 60Hz (1 cycle). Line events typically last roughly 6 cycles (1/10 second) as in the fault illustrated in Figure 2, although some faults last substantially longer. Because the events we are interested in are characterized more by the voltage's deviation from its normal operating point than by the shape of the voltage curve, we treat classification as an episodic task and do not process the data as a time series. Instead, for all the classifiers described in this paper, classification occurs at each time step independently from other time steps. Thus, one minute of data yields 3600 (60 seconds

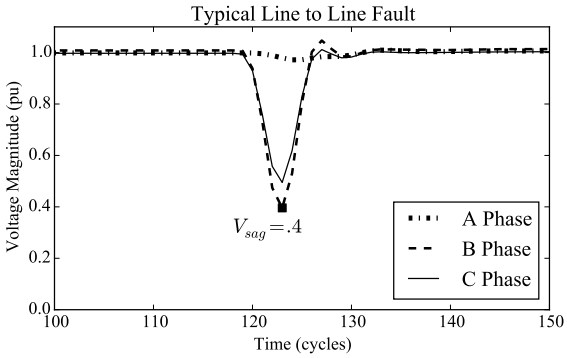

Fig. 2. Per-unit voltage magnitudes and sag voltage during a fault

$\times$ 60 samples per second) possible classification results.

After optimizing the arrangement of the attribute tests, the expert's hand-built classification rules can be used to create a decision tree containing thirteen nodes, five of which are leaves indicating the classification results of *SLG*, *LL*, *3P* or *No Fault* (two distinct *No Fault* leaves exist in the tree). Prior to performing any tests with the hand-built classification rules, per-unit voltages for each phase are calculated and then sorted in increasing order. These three sorted per-unit voltages constitute the only features tested by the hand-built rules. Once a fault type has been identified, the position of each named phase (A,B,C) in the sorted order can be used to identify the specific faulted phase(s) if desired.

Although the hand built classification rules accurately identify fault types when used at locations nearest to a given fault, the method of setting thresholds by manually examining voltage plots does not scale well. Our current data set includes 44 PMUs and the domain expert worked with plots showing voltage curves and measurements from all PMUs adjacent to each fault location (typically 2-5 PMUs). In total, this amounted to hundreds of pages of data to examine. Scaling this job even by a factor of 10 (for example to incorporate plots from all the PMUs in our dataset) would be extremely difficult without resorting to a statistical approach or to machine learning. However, because the power industry is extremely conservative when it comes to adopting new technologies, machine learning is still not routinely applied to real PMU data streams. As a first step in that direction, we aim to explore the feasibility of replacing the hand-coded domain-expert's rules with a classifier built using machine learning techniques.

IV. Methodology

To evaluate the feasibility of replacing hand-built classification rules with a learned classifier, we begin by identifying relevant performance metrics for our study and then discuss details of our training set. In Section V-A we establish the baseline performance of our hand-built classification rules. Then, in Section V-B we apply decision tree learning to a set of features similar to those used for the hand-built rules. In Section V-C, we transform these initial features in an effort to improve robustness of the classifier and study the effect. In both experiments, we also explore lifting the constraint imposed on the hand-built rules of using the classifier at a bus located near the fault. Learning a decision tree that supports fault identification from across the grid is a more challenging task because the fault signatures get less distinct as one moves further from the fault's origin and because substantially more data must be processed during the learning task. However, the benefit of this approach is improved classification robustness in the face of PMU failure or network error.

A. Metrics

To evaluate the quality of our classifiers, we propose an evaluation scheme that includes the following metrics:

- **Boolean Classification:** At the highest level of abstraction, we are interested in a classifier that correctly distinguishes fault conditions from normal operation. To gauge this, we propose to examine the boolean classification quality via accuracy, precision, recall (sensitivity) and specificity in this two-class setting. We will further distinguish between performance at the fault location and across other (more distant) PMU sites as appropriate.
- **Type-Specific Classification:** A classifier that correctly identifies a fault condition should ideally continue to distinguish between each of the three fault types (Single Line to Ground, Line to Line, and Three Phase faults) described previously. To this end, we propose to measure accuracy across the four fault/normal classes as well as macro-averaged precision and recall (sensitivity) across the type-specific fault classes. As with boolean classification, these measurements are assessed both at the fault location and across all other PMU sites.
- **Site Redundancy:** Since the grid is interconnected, activity at one location impacts activity at other locations. A robust classifier should be able to identify a fault signature not just at the site where it occurs, but from the PMU data observed across a relatively wide subset of the grid. To measure this effect, we propose to examine the number of PMU signals correctly classifying each event. Two values: the median and the fifth percentile value are used to evaluate performance. For each fault, we determine the number of PMU signals correctly classifying that event. From this list, we find the median and fifth percentile values. 50% of the events are correctly recognized by the former (median value) number of PMU signals while 95% of the events are correctly recognized by the later (fifth percentile) number of PMU signals.

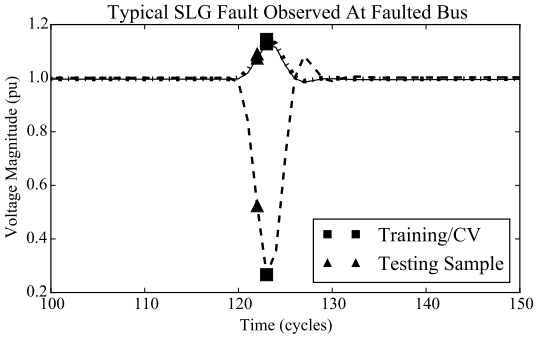

Fig. 3. Per-phase voltages during a typical event

B. Training and Testing Data

Our training and testing data sets consist of instances representing both faults and normal operation. Instances are created from (transformed) measurements of the three voltage phases (A,B,C) at a specific moment in time and measurements of the steady state voltage for each of the phases. From time to time, some PMUs may be non-operational, or some signals from a specific PMU may be missing from the data set. Valid classification instances (training or testing) can only be created when we can collect a set of non-zero measurements from all three voltage phases and also obtain a steady state measurement from that voltage phase.

Figure 3 illustrates a typical Single Line to Ground fault (SLG), where one of the phases show a significant voltage sag, and the voltage levels of the other two phases are largely unaffected. These line faults typically occur on a transmission line connecting two substations, although at times they can also occur at the substation itself. Note that although the event list that BPA provided contains 60 faults, in this study, we only use the faults which occur in an area where PMUs are deployed and currently operational. In other words, faults are excluded from our dataset if there is no valid data from a PMU in the neighborhood of the fault. For example, assume a fault occurs on the line connecting sites 38 and 27 in Figure 1. The neighborhood for this fault includes the PMUs placed at sites 38 and 27 as well as the PMUs immediately adjacent to those sites (i.e., 46, and 45; 26 is also in the neighborhood, but does not have a PMU). Three of the original 60 faults described in Section III have no PMUs in the neighborhood of the fault location, leaving 57 valid faults for our data set.

Using the method outlined in Liang et al [29] on these 57 faults, we find the PMU whose voltage experiences the largest deviation from its steady state value where steady state is measured by the median voltage in the 20 cycles prior to the fault. This is termed the PMU *at the fault location*[1]. We then use the moment in time where this PMU experiences the largest deviation from steady state to sample the individual A, B and C voltage phases (squares in Figure 3). These measurements form the training instance representing that specific fault *at the fault location*. Next, we sample this same moment in time from all voltage signals across the grid. If

[1]When checked against BPA's dispatch notes related to each of the 57 faults in our data set, the PMU at the fault location is always a PMU directly connected to the line experiencing the fault (e.g., site 38 or 27 from the example above) when PMUs on *both sides* of the line are operational.

we obtain valid signals from all three phases along with valid steady sate measurements we can form an additional training instance for this fault from the grid at large. Since most PMUs measure three phase voltages at multiple locations within a single substation and since some PMUs also measure three phase voltages on transmission lines, for any given fault we can typically generate more training instances than there are operational PMUs.

Fault instances in our test set are produced from the same 57 faults, but at the cycle preceding the moment of time used to generate the training instances (triangles in Figure 3). Although these samples are not entirely independent of the training data, they were not used for cross-validation or any other purpose during the development of the classifiers discussed below. Thus, we believe that these points serve as a reasonable proxy for new archival data with unseen faults. Indeed, they may even be a more challenging test than new events since the selection methodology ensures that they will typically be smaller deviations from steady state than the points used in training.

In total, this method of selecting training and testing instances yields two sets with identical size, each containing 4,533 elements. Of these, 4,135 are SLG faults, 348 are LL faults and 50 are 3P faults. To these sets, we add instances selected from roughly 800 minutes of normal operation over the one year period. Like fault instances, normal instances are created from measurements of 3-phase voltages and associated steady state values. For each of the 800 minutes of normal data, and each valid voltage signal measured by some PMU, we tracked the minimum and maximum deviation from the per-minute median (an approximation of steady state voltage). These points in time, where the largest deviations from steady state occur under normal operating conditions, and two additional, randomly selected times from within each minute, were used to create the training instances representing "normal" operation. In total, this approach yields 17,662 instances representing normal operation. We randomly selected half (8,831) of these normal samples to use for training, leaving the other half for testing. Therefore, our training and testing data sets each contain 13,364 instances of both normal operation and fault conditions.

V. Evaluation

In this section, we examine the performance on the testing dataset of the expert's hand-built classification rules as compared to similar rules built using J48. We show that machine learning can achieve results similar to the expert for classification at the fault location. More importantly, because we can process a substantially larger dataset using automated methods, machine learning can help achieve a more robust classifier when data is examined across the grid as a whole.

A. Baseline: Hand-Built Classification Rules

To establish a baseline for performance, we evaluated the hand-built classification rules using the 57 faults discussed in Section IV. It is important to note that while the hand-built rules were not built explicitly using these training samples, the expert was given graphs for the entire fault duration as it appeared near the faulted location as well as the p.u. voltages for the moment in time with the largest deviation from steady state. Since the training examples are voltage measurements obtained during the moment of greatest voltage deviation during the fault, the data provided to the expert contained the same information as the training set with two exceptions: (1) the expert had access to the time series data near the fault (a duration that included roughly 10 cycles (1/6 second) before and after each fault); (2) the expert had access to voltage readings from PMUs located closest to each fault (typically about two sites) instead of at all functioning PMUs.

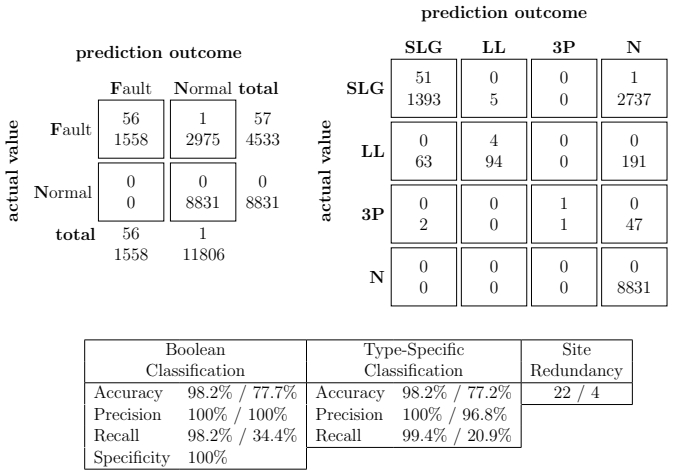

Boolean Classification		Type-Specific Classification		Site Redundancy
Accuracy	98.2% / 77.7%	Accuracy	98.2% / 77.2%	22 / 4
Precision	100% / 100%	Precision	100% / 96.8%	
Recall	98.2% / 34.4%	Recall	99.4% / 20.9%	
Specificity	100%			

Fig. 4. Test set performance of hand-built classification rules.

Figure 4 illustrates the performance of the hand-built classification rules. The confusion matrix on the left side illustrates the *boolean* classification performance: the ability to distinguish between faults and normal operation. The confusion matrix on the right side of the figure illustrates the performance on *type-specific* fault classification. Cells in both confusion matrices hold two values. The top value indicates the count *at the fault location* as defined in Section IV-B. The bottom value indicates the count *across the grid as a whole* (including the site nearest to the fault location).

The type-specific classification performance (right confusion matrix) includes each of the three fault classes *and* normal operation. The type-specific 3x3 sub-matrix that includes rows and columns SLG, LL, and 3P sum to the entry in the upper-left corner of the boolean confusion matrix (true positives) while the values in the column labeled N sum to the value in the upper-right corner (false negatives) of the boolean confusion matrix. Again, cells hold two values: counts associated with the PMU site nearest to the fault, and counts associated with the grid as a whole.

The table below the confusion matrices illustrates the scalar valued performance measures. For the boolean classification task, we have indicated accuracy, precision, recall and specificity. While it is logical to measure accuracy, precision, and recall at the location of each fault (where the voltage signature of the event should be most prominent), specificity is measured only across the grid as a whole since non-fault data points do not have a reference location in the same way as fault data points do. For the type-specific classification task, we indicate accuracy, precision and recall. Note that accuracy in the type-specific context counts true positives of all four classes (faults

and non-faults) and divides by the sum of all examples (at the fault location or at large). In this multi-class setting, we compute precision and recall by macro-averaging across the fault types (SLG, LL, TP). The normal class (N) is excluded from the type-specific precision/recall macro-averages since these scores are intended to highlight the ability to distinguish between each of the individual fault types. Finally, the last column of the table indicates median and fifth percentile site redundancy (larger values indicate the fault is more reliably detected across the grid). For these hand-built rules, accuracy is very high at the fault location, but suffers when measured across the grid at large. Specificity and precision are high in all cases because of the extremely low number of false positives that comes from basing the thresholds on the signals nearest to the fault location. However, this also results in very low recall when sites distant from the fault are considered.

B. Decision Trees With Expert Derived Features

As a first step towards replacing the domain expert's hand-coded rules described in Section III, we used Weka's [30] J48 [31] decision tree learner to infer the classification rules using the features readily available to the domain expert. In particular, we used both per-phase steady state, sag voltages, and sag voltages normalized by their steady state values (p.u.). We examined these measurements when arranged by named phase (e.g., the A, B, and C-phase sag voltages) and when arranged by the relative order of their deviation from steady state (e.g., the primary, secondary and tertiary sag values). This later representation leverages symmetry within each fault type (Single Line to Ground faults will have one significant sag, Line to Line faults two, etc).

Although J48 is rarely considered the most sophisticated learning algorithm, we have chosen it here for two specific reasons. First, J48 produces a classifier that is directly comparable to the hand-built classification rules both in terms of performance *and* in terms of hypothesis complexity. Specifically, we can compare the size of the decision trees formed by the expert's rules with the size of the decision tree produced algorithmically. Second, unlike other classifiers such as support vector machines, decision trees have the benefit of being easily interpreted, analyzed, and validated by human experts. In a domain such as power systems where new technology is adopted relatively slowly, we believe that this property can help foster acceptance.

Figure 5 illustrates the performance of the decision tree built using the features described above. Performance generally improves for the binary classification task compared to the hand-built classification rules, but type-specific recall suffers greatly since no Three Phase faults are identified. As a result, precision is macro-averaged over only the two remaining fault categories (it is undefined for the Three Phase class), yet precision still remains below the level of the hand-built rules for measurements taken at the fault location. For measurements at a distance, recall, accuracy and site redundancy all improve dramatically compared to the hand-built rules. However, the tree produced using these features is relatively large and contains 21 nodes including 11 leaves compared against the decision tree built using the expert's rules which contained 13 nodes (five of which were leaves).

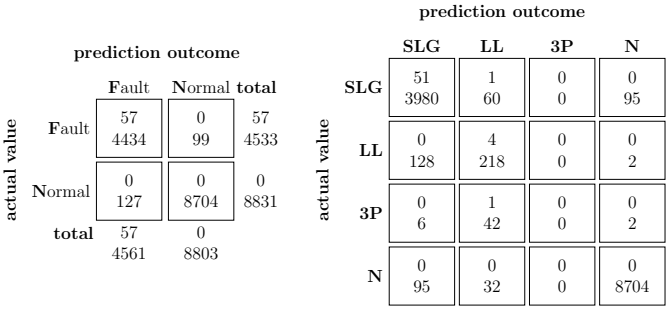

Boolean Classification		Type-Specific Classification		Site Redundancy
Accuracy	100% / 98.3%	Accuracy	96.5% / 96.5%	78 / 48
Precision	100% / 97.2%	Precision	83.3% / 78.2%	
Recall	100% / 97.8%	Recall	66.0% / 53.0%	
Specificity	98.6%			

Fig. 5. Test set performance of decision tree using expert's feature set

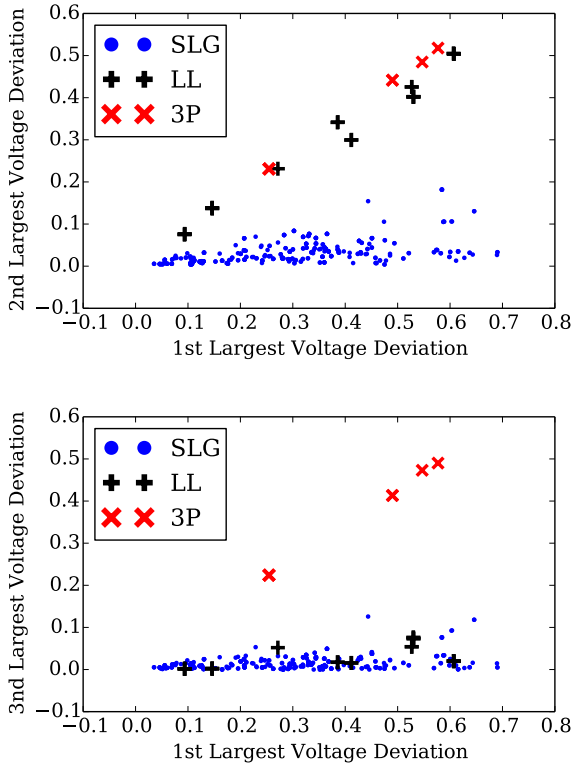

Fig. 6. Sorted phase deviation from steady state *at fault location*

C. Decision Trees With Novel Features

Although the performance of our first decision tree is not unreasonable, most of the trees produced during our exploration of the hypothesis space seemed to have more internal nodes than was easily justified. This observation is not unexpected as J48 is well known to be prone to overfitting. Plots of the dominate features in Figure 6 and Figure 7 illustrate a source of the problem. The plot shows the first, second, and third largest voltage deviations away from steady state when normalized by steady state values. The plots in Figure 6 show these features when viewed for faults *at the*

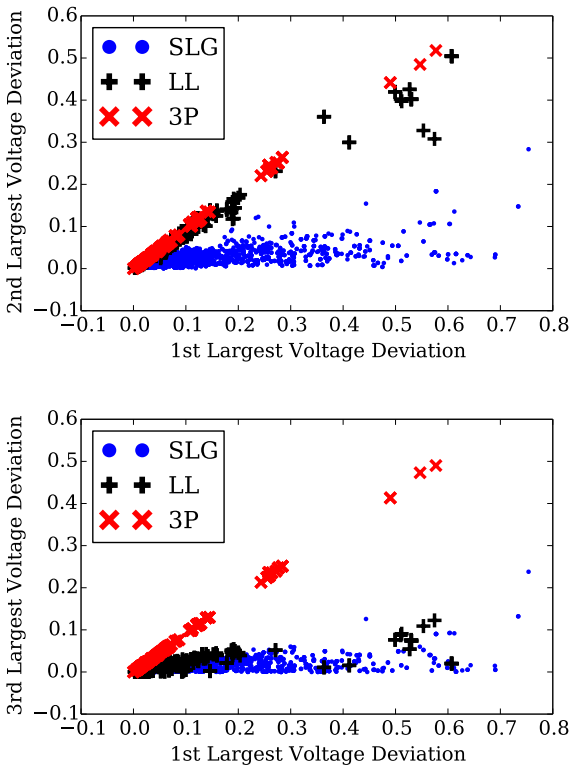

Fig. 7. Sorted phase deviation from steady state *across all PMU locations*

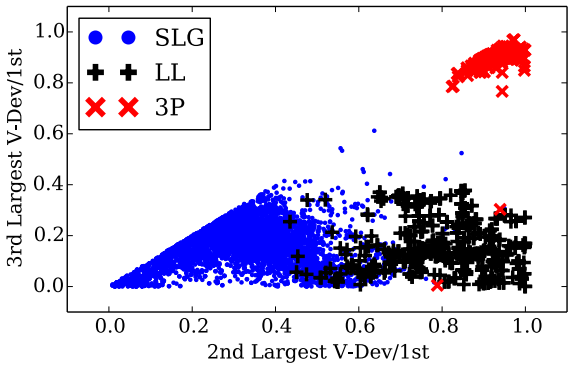

Fig. 8. Relative deviation from steady state of sorted phases (across all PMUs)

fault location. Here, we see that the different event types can be separated, although no single pair of features is sufficient to separate all three types into individual clusters. As we move to view the events from across all PMUs (Figure 7), however, we can see that all three event types converge around $(0.0, 0.0)$ in both plots. These plots show that as we move away from the fault location to more remote PMUs the voltage disturbance is less pronounced (it approaches zero). This represents a potential problem for differentiating event types at a distance.

To improve recognition at a distance, we explored a transformed feature space illustrated in Figure 8. Here, deviation from steady state is ordered (largest deviation first) and then normalized with respect to the largest deviation. Now, these

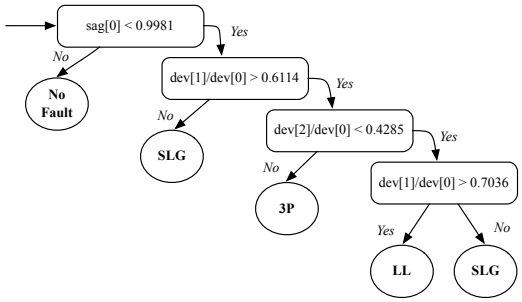

Fig. 9. Improved decision tree using relative deviation, a novel feature (*sag*: p.u. voltages of each phase in increasing order; *dev*: absolute value voltage changes from steady state measured in p.u., arranged in decreasing order.)

prediction outcome

actual value	Fault	Normal	total
Fault	57 4434	0 99	57 4533
Normal	0 127	0 8704	0 8831
total	57 4561	0 8803	

prediction outcome

actual value	SLG	LL	3P	N
SLG	51 4011	0 22	1 7	0 95
LL	0 67	4 279	0 0	0 2
3P	0 0	0 0	1 48	0 2
N	0 65	0 17	0 45	0 8704

Boolean Classification		Type-Specific Classification		Site Redundancy
Accuracy	100% / 98.3%	Accuracy	98.2% / 97.6%	81 / 49
Precision	100% / 97.2%	Precision	83.3% / 77.5%	
Recall	100% / 97.8%	Recall	99.4% / 91.1%	
Specificity	98.6%			

Fig. 10. Test set performance of relative deviation decision tree

two features represent the relative size of the second and third deviations relative to the first. As expected, this plot shows a much improved separation of the event types when viewed from the perspective of any PMU on the grid. The decision tree learned with these features contains only 9 nodes, 5 of which are leaves: it is illustrated in Figure 9. We refer to this tree as the "relative deviation" decision tree.

Figure 10 shows the performance of the relative deviation decision tree on these fault types. In particular, it is worth noting that at the fault location, performance on the training set in terms of accuracy and recall meets or exceeds that of the hand-built rules. In addition, accuracy and recall vastly improve for measurements made from across the grid as do both site redundancy scores. Type-specific precision is reduced both at the fault location and across the grid, but this seems a reasonable tradeoff since the boolean classification precision is still very high (reduced only by 2.8% from the expert's rules when examining observations from across the grid). Moreover, the main concern from a low precision (which would be due to false positives) would be a false positive rate that was too high to make the classifier useful in any practical setting. However, our classifier still obtains very high specificity score indicating that the number of (boolean) false positives, is still just a small fraction of all the normal data being examined.

VI. Conclusion

The development of the smart grid presents many new opportunities to leverage advances in computer science and machine learning to improve robust operation, fault detection and control of the grid. In this paper, using PMU data collected from BPA's operational power grid during one a year period, we have demonstrated that machine learning can be used to perform line-event detection with performance that is similar to a domain expert's hand-built classification rules when applied to signals located near a fault. At the same time, because machine learning is able to leverage much more data during training, we were able to demonstrate superior performance as compared to the hand built rules when classifying events from a distance. As the number of deployed PMUs increases, the benefits of applying machine learning techniques to smart grid operation will likely continue to grow.

Work is ongoing in several directions. First, we are examining other learning algorithms for event classification, such as support vector machines. Second, besides supervised learning, we are also applying unsupervised clustering techniques to PMU data, aiming to identify unknown events and signatures. Finally, we are repurposing these machine learning techniques to solve different problems in the power grid domain, e.g., data cleansing and spoofed signal detection.

References

[1] N. B. Bhatt, "Role of synchrophasor technology in the development of a smarter transmission grid," in *Power and Energy Society General Meeting, 2010 IEEE*. IEEE, 2010, pp. 1–4.

[2] A. Phadke, "Synchronized phasor measurements - a historical overview," in *Transmission and Distribution Conference and Exhibition 2002: Asia Pacific. IEEE/PES*, vol. 1, Oct 2002, pp. 476–479.

[3] E. Schweitzer, D. Whitehead, G. Zweigle, and K. G. Ravikumar, "Synchrophasor-based power system protection and control applications," in *63rd Annual Conference for Protective Relay Engineers*. IEEE, 2010, pp. 1–10.

[4] IEEE, "IEEE standard for synchrophasor data transfer for power systems," *IEEE Std C37.118.2-2011 (Revision of IEEE Std C37.118-2005)*, pp. 1–53, Dec 2011.

[5] D. Elizondo, R. M. Gardner, and R. Leon, "Synchrophasor technology: The boom of investments and information flow from north america to latin america," in *Power and Energy Society General Meeting, 2012 IEEE*. IEEE, 2012, pp. 1–6.

[6] M. Patel, S. Aivaliotis, E. Ellen *et al.*, "Real-time application of synchrophasors for improving reliability," *NERC Report, Oct*, 2010.

[7] A. Silverstein and J. E. Dagle, "Successes and challenges for synchrophasor technology: An update from the north american synchrophasor initiative," in *45th Hawaii International Conference on System Science (HICSS 2012)*. IEEE, 2012, pp. 2091–2095.

[8] W. Premerlani, B. Kasztenny, and M. Adamiak, "Development and implementation of a synchrophasor estimator capable of measurements under dynamic conditions," *IEEE Transactions on Power Delivery*, vol. 23, no. 1, pp. 109–123, Jan 2008.

[9] P. Pourbeik, P. S. Kundur, and C. W. Taylor, "The anatomy of a power grid blackout," *IEEE Power and Energy Magazine*, vol. 4, no. 5, pp. 22–29, 2006.

[10] B. Ravindranath, *Power System Protection and Switchgear*. Wiley Eastern Limited, 1977. [Online]. Available: https://books.google.com/books?id=I3N4aQwfSr4C

[11] Y. Hu and D. Novosel, "Challenges in implementing a large-scale pmu system," in *International Conference on Power System Technology*, Oct 2006, pp. 1–7.

[12] M. Kezunovic, L. Xie, and S. Grijalva, "The role of big data in improving power system operation and protection," in *2013 IREP Symposium Bulk Power System Dynamics and Control - IX Optimization, Security and Control of the Emerging Power Grid (IREP)*, Aug 2013, pp. 1–9.

[13] J.-A. Jiang, J.-Z. Yang, Y.-H. Lin, C.-W. Liu, and J.-C. Ma, "An adaptive pmu based fault detection/location technique for transmission lines. i. theory and algorithms," *IEEE Transactions on Power Delivery*, vol. 15, no. 2, pp. 486–493, Apr 2000.

[14] G. Liu and V. Venkatasubramanian, "Oscillation monitoring from ambient pmu measurements by frequency domain decomposition," in *IEEE International Symposium on Circuits and Systems (ISCAS 2008)*, May 2008, pp. 2821–2824.

[15] G. Chang, J.-P. Chao, H.-M. Huang, C.-I. Chen, and S.-Y. Chu, "On tracking the source location of voltage sags and utility shunt capacitor switching transients," *IEEE Transactions on Power Delivery*, vol. 23, no. 4, pp. 2124–2131, Oct 2008.

[16] J. E. Tate and T. J. Overbye, "Line outage detection using phasor angle measurements," *IEEE Transactions on Power Systems*, vol. 23, no. 4, pp. 1644–1652, 2008.

[17] P. Trachian, "Machine learning and windowed subsecond event detection on PMU data via Hadoop and the openPDC," in *Proceedings of the IEEE Power and Energy Society General Meeting*, 2010, pp. 1–5.

[18] S. Rusitschka, K. Eger, and C. Gerdes, "Smart grid data cloud: A model for utilizing cloud computing in the smart grid domain," in *First IEEE International Conference on Smart Grid Communications (SmartGridComm)*, Oct 2010, pp. 483–488.

[19] O. Antoine and J.-C. Maun, "Inter-area oscillations: Identifying causes of poor damping using phasor measurement units," in *Power and Energy Society General Meeting, 2012 IEEE*. IEEE, 2012, pp. 1–6.

[20] Y.-G. Zhang, Z.-P. Wang, J.-F. Zhang, and J. Ma, "Fault localization in electrical power systems: A pattern recognition approach," *International Journal of Electrical Power & Energy Systems*, vol. 33, no. 3, pp. 791–798, 2011.

[21] R. Diao, K. Sun, V. Vittal, R. O'Keefe, M. Richardson, N. Bhatt, D. Stradford, and S. Sarawgi, "Decision tree-based online voltage security assessment using pmu measurements," *IEEE Transactions on Power Systems*, vol. 24, no. 2, pp. 832–839, May 2009.

[22] P. K. Ray, S. R. Mohanty, N. Kishor, and J. P. Catalão, "Optimal feature and decision tree-based classification of power quality disturbances in distributed generation systems," *IEEE Transactions on Sustainable Energy*, vol. 5, no. 1, pp. 200–208, 2014.

[23] R. Salat and S. Osowski, "Accurate fault location in the power transmission line using support vector machine approach," *IEEE Transactions on Power Systems*, vol. 19, no. 2, pp. 979–986, May 2004.

[24] F. R. Gomez, A. D. Rajapakse, U. D. Annakkage, and I. T. Fernando, "Support vector machine-based algorithm for post-fault transient stability status prediction using synchronized measurements," *IEEE Transactions on Power Systems*, vol. 26, no. 3, pp. 1474–1483, 2011.

[25] C. Zheng, V. Malbasa, and M. Kezunovic, "Regression tree for stability margin prediction using synchrophasor measurements," *IEEE Transactions on Power Systems*, vol. 28, no. 2, pp. 1978–1987, 2013.

[26] M. He, V. Vittal, and J. Zhang, "Online dynamic security assessment with missing pmu measurements: A data mining approach," *IEEE Transactions on Power Systems*, vol. 28, no. 2, pp. 1969–1977, 2013.

[27] M. Al Karim, M. Chenine, K. Zhu, and L. Nordstrom, "Synchrophasor-based data mining for power system fault analysis," in *3rd IEEE PES International Conference and Exhibition on Innovative Smart Grid Technologies (ISGT Europe 2012)*. IEEE, 2012, pp. 1–8.

[28] J. Milanovic, K. Yamashita, S. Martinez Villanueva, S. Djokic, and L. Korunovic, "International industry practice on power system load modeling," *Power Systems, IEEE Transactions on*, vol. 28, no. 3, pp. 3038–3046, Aug 2013.

[29] X. Liang, S. Wallace, and X. Zhao, "A technique for detecting wide-area single-line-to-ground faults," in *2nd IEEE Conference on Technologies for Sustainability (SusTech 2014)*, 2014.

[30] M. Hall, E. Frank, G. Holmes, B. Pfahringer, P. Reutemann, and I. H. Witten, "The weka data mining software: An update," *SIGKDD Explorations Newsletter*, vol. 11, no. 1, pp. 10–18, Nov. 2009.

[31] R. Quinlan, *C4.5: Programs for Machine Learning*. San Mateo, CA: Morgan Kaufmann Publishers, 1993.